RSC Advances

ROYAL SOCIETY OF CHEMISTRY

www.rsc.org/advances

Journal Name

ARTICLE

Modification of Eu^{3+}-beta-diketonate complex-intercalated Laponite with a terpyridine-functionalized ionic liquid

Received 00th January 20xx,
Accepted 00th January 20xx

DOI: 10.1039/x0xx00000x

www.rsc.org/

Yalan Yao, Zhiqiang Li and Huanrong Li*

Lanthanide complex-based organic-inorganic hybrid material with intense luminescence has been obtained by modifying the Eu^{3+}-beta-diketonate complex-intercalated Laponite with a terpyridine moiety-functionalized ionic liquid. Remarkable luminescence enhancement as well as improved thermal- and photo- stability were observed after modification with the functional ionic liquid. The ionic liquid is believed to coordinate to and sensitize Eu^{3+} ions as well as decrease proton concentration on Laponite surfaces.

1. Introduction

To date, lanthanide complexes based luminescent inorganic–organic hybrid materials have attracted the attention of researchers across various disciplines due to the rich applications, such as display, lighting, optical devices and medical technology.[1-10] Such luminescent materials typically are prepared by doping lanthanide complexes into various matrices including zeolites,[11-13] polymers,[14] mesoporous silica,[15] titania,[16, 17] xerogels[18], and clay materials[19-21]. As the existing literatures illustrated, lanthanide complexes encapsulated in matrix lead to a better optical properties and higher stability compared with the individual lanthanide complexes. As synthesized clay, Laponite has a layered structure with expandable interlayer spaces and favourable cation-exchange capacity, which can be completely exfoliated in water.[22-24] These inherent properties make it a suitable host for incorporation of lanthanide complexes in aqueous solution to form luminescent hybrid materials. However, abundant acidic sites exist on the surface of the individual delaminated platelets of Laponite in water, which have negative influence on the luminescence efficiency.[25, 26] For instance, the luminescence efficiency of terbium complexes ($Tb(bpy)_2^{3+}$) on the platelets of Laponite appears to be rather low.[26] Fortunately, Yang *et al* observed a significant increase in the luminescence efficiency of hybrids consisting of Eu^{3+}-beta-dikeonate and Laponite after adding imidazolium salt, which has been ascribed to the decreasing of the proton activity on clay surface by the added imidazolium salt that act through a mechanism of synergic effect of ion exchange and neutralization.[27] Other ionic liquids even displaying acidity in water can also enhance the luminescence of such kind of hybrid materials due to their capacity of removing proton via ion exchanges. [27]

Encouraged by this, herein, we report the luminescence enhancement of hybrid materials consisting of Eu^{3+} (tta_n) complex (tta= 2-Thenoyltrifluoroacetone) and the inorganic matrix Laponite upon modification with a terpyridine moiety-containing ionic liquid (tpy-IL),[28] which is believed to act both as a sensitizer for Eu^{3+} ions and as an proton exchanger for decreasing the proton concentration on Laponite surfaces. In addition, improved thermal- and photo-stability of the tpy-IL modified hybrid materials can also be observed.

2. Results and Discussion

Laponite RD (chemical composition $Na_{0.7}[Si_8Mg_{5.5}Li_0O_{20}(OH)_4]$) is a layered smectite-type clay with stacked platelets average dimension of 1 nm × 25 nm. It is well known that Laponite is completely delaminated to individual disks to form transparent solution after swelling in water. Each single Laponite platelet contains roughly 1500 unitary cells (u. c.). In consequence, counter cations such as Na^+ are accessible to ion exchange and organic species can be easily inserted in the interlayer.[23, 29] According to the supplier, Laponite has a cation exchange capacity (CEC) of 50–60 meq/100 g, i.e. about 55–65% of the existing Na^+ ions.[20, 22, 30, 31] The mean layer charge of Laponite determined using the n-alkylammonium method is 0.346.[32-34] In this study, the intercalation of Eu^{3+}-beta-diketonate complexes within the Laponite was achieved by a two-step procedure according to our previous work. Firstly, material of Eu^{3+}@LA were prepared by substituting the positive Na^+ ions of Laponite with Eu^{3+} via ion exchanges in aqueous solution, followed by addition of ethanol solution of tta. We find 80% of the available Na^+ ions are exchanged by Eu^{3+} ions (through analyzing the supernatant titration against EDTA). As a result, the final experimentally determined tta and Eu^{3+} loading per

Y. Yao. Dr. Z. Li. Prof. Dr. H. Li.
School of Chemical Engineering and Technology
Hebei University of Technology
GuangRong Dao 8, Hongqiao District
Tianjin 300130, P. R. China.
**Corresponding author e-mail address:* lihuanrong@hebut.edu.cn

u.c. under this condition is ~1 and ~0.352, respectively.[27] The presence of the tta ligand can be detected by UV-vis absorption according to the procedure.[35] As shown in Fig. 1c, the $Eu^{3+}(tta_n)$@LA exhibited characteristic emission of Eu^{3+} when irradiated by near UV light, this phenomenon indicate the formation of Eu^{3+}-beta-diketonate complexes in between the interlayers of Laponite. After the insertion of tpy-IL, the luminescence enhancement was observed by naked eyes in the obtained $Eu^{3+}(tta_n)$@LA/tpy-IL. The influence of the ionic liquid in the hybrid materials is especially obvious, which shows bright red emission (Fig. 1d).

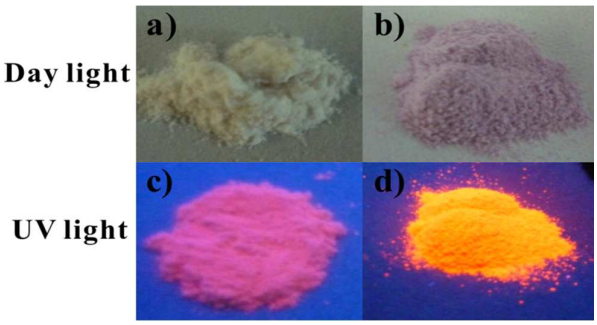

Fig. 1. Digital photos of the samples; a) $Eu^{3+}(tta_n)$@LA (day light), b)$Eu^{3+}(tta_n)$@LA/tpy-IL (day light); c) $Eu^{3+}(tta_n)$@LA (UV light), d)$Eu^{3+}(tta_n)$@LA/tpy-IL (UV light).

2.1 X-ray diffraction

The formation of luminescent hybrid materials based on Laponite was confirmed by the powder X-ray diffraction (XRD) (Fig. 2). All the samples exhibit a somewhat broad diffraction pattern, indicating a rather pronounced stacking disorder and the small crystallites particle size of the samples.[36] The broad diffraction pattern at approximately 2θ=5.89° is attributed to the (001) crystal plane or the basal spacing of Laponite (Fig. 2a and idealized structure formula of Laponite).[19]

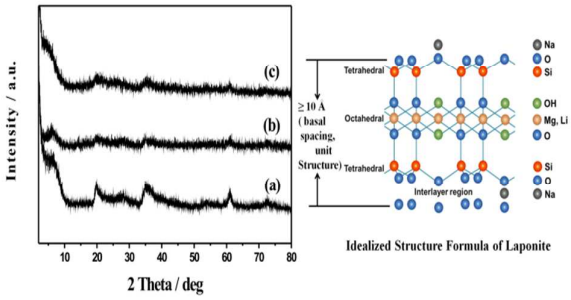

Fig. 2. XRD patterns of a) LA, b) $Eu^{3+}(tta_n)$@LA and c) $Eu^{3+}(tta_n)$@LA/tpy-IL (left), idealized structure formula of Laponite (right).

As shown in Fig. 2b, the basal spacing of Laponite expanded from approximately 15 Å to 16.4 Å after the accommodation of Eu^{3+}-beta-diketonate complexes, and implied that at least a proportion of tta complexes were intercalated within the interlayers of Laponite. The basal spacing of Laponite in $Eu^{3+}(tta_n)$@LA/tpy-IL increased from approximately 15 Å to 18.5 Å (Fig. 2c), indicating that tpy-IL has been located the interlayer space of Laponite. Nevertheless, the location of guest complexes on external adsorption sites on Laponite could not be excluded.

2.2 FT-IR spectra and SEM

The modification of tpy-IL with $Eu^{3+}(tta_n)$@LA can be further confirmed by the FTIR spectra. Fig. 3 displays the FTIR spectra of $Eu^{3+}(tta_n)$@LA (a) and $Eu^{3+}(tta_n)$@LA/tpy-IL (b). Bands centered at about 1607, 1587, and 1563 cm^{-1} are assigned to the imidazole ring and the pyridine ring of tpy-IL.[37, 38] Upon modification of tpy-IL with the hybrid material $Eu^{3+}(tta_n)$@LA , these bands appears in spectrum(b) and the shift of some absorption bands corresponding to the terpyridine moieties also can be observed, which indicates a successful formation of $Eu^{3+}(tta_n)$@LA/tpy-IL. The morphology of the $Eu^{3+}(tta_n)$@LA and $Eu^{3+}(tta_n)$@LA/tpy-IL was characterized by SEM experiment. As shown in Fig. 4a, a number of uniform size nanoparticles with an average diameter of 40-50 nm were observed in SEM image. Similar morphology with larger size nanoparticles was observed in the SEM image of $Eu^{3+}(tta_n)$@LA/tpy-IL (Fig. 4 b).

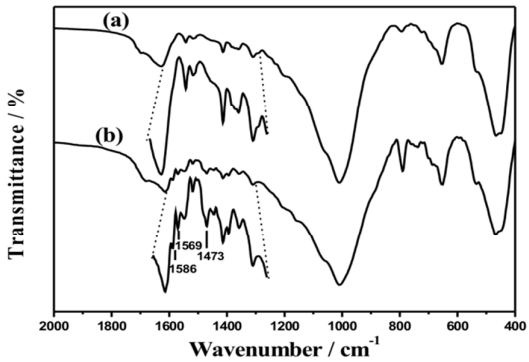

Fig. 3. FTIR spectra of (a) $Eu^{3+}(tta_n)$@LA and (b) $Eu^{3+}(tta_n)$@LA/tpy-IL.

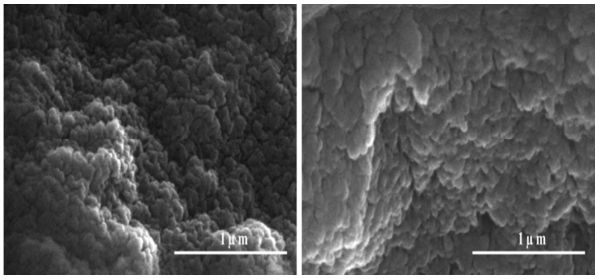

Fig. 4. The scanning electron micrographs for (a) $Eu^{3+}(tta_n)$@LA and (b) $Eu^{3+}(tta_n)$@LA/tpy-IL.

2.3 Optical properties

We find that the luminescence performance of $Eu^{3+}(tta_n)$@LA/tpy-IL is significant influenced by the initial addition amount of tpy-IL. The luminescence intensity of $Eu^{3+}(tta_n)$@LA/tpy-IL increased gradually with increasing amount of tpy-IL, which reached its maximum when the quality ratio of tpy-IL to $Eu^{3+}(tta_n)$@LA was set as 1:1 (Fig. 5). Therefore, the initial amount of tpy-IL to $Eu^{3+}(tta_n)$@LA was maintained at 1:1 in the following experiments. The amount of tpy-IL actually loaded on the $Eu^{3+}(tta_n)$@LA/tpy-IL hybrid materials was determined by elemental analysis. We found that the loaded amount of tpy-IL is about 0.225/u.c..

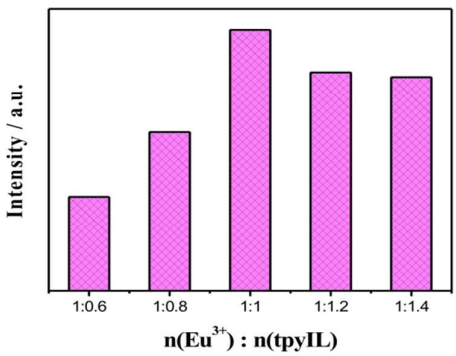

Fig. 5. Luminescence intensity at 612 nm versus the amount of tpy-IL initially added to $Eu^{3+}(tta_n)$@LA.

Further support is gained from the optical spectra as shown in Fig. 6. Both $Eu^{3+}(tta_n)$@LA and $Eu^{3+}(tta_n)$@LA/tpy-IL materials show similar excitation and emission spectra, the excitation spectra are composed of a broad band from 200 to 400 nm resulting from the absorption of ligands. The excitation of the $Eu^{3+}(tta_n)$@LA is rather low over the monitored spectral range. Nevertheless, introduction of tpy-IL into the $Eu^{3+}(tta_n)$@LA materials leads to a remarkable excitation enhancement peaked at approximately 370nm. Characteristic luminescence of Eu^{3+} located at 579 ($^5D_0/^7F_0$), 592 ($^5D_0/^7F_1$), 612 ($^5D_0/^7F_2$), 652 ($^5D_0/^7F_3$) and 698 ($^5D_0/^7F_4$) nm was observed both in $Eu^{3+}(tta_n)$@LA and $Eu^{3+}(tta_n)$@LA/tpy-IL under excited at 350 nm(Fig. 6b). However, $Eu^{3+}(tta_n)$@LA show relatively weak characteristic luminescence of Eu^{3+}, obvious improvement in luminescence intensity is observed upon the incorporation of tpy-IL. Apparently, the spectrum is dominated by the hypersensitive transition $^5D_0 \rightarrow {}^7F_2$, resulting in bright red luminescence. The integrated intensity of $^5D_0/^7F_2$ transition of $Eu^{3+}(tta_n)$@LA/tpy-IL was 10 times than that of $Eu^{3+}(tta_n)$@LA.

The remarkable luminescent enhancement in $Eu^{3+}(tta_n)$@LA/tpy-IL can be explained as follows. The addition of tpy-IL can fully protect Eu^{3+} ions from the water molecules quenching and remove the abundant protons on the Laponite platelets. The number of water molecules in the coordination sphere of Eu^{3+} was evaluated based on the emission spectra and the life time of the $^5D_0$ state of the Eu^{3+} ions according to the method described elsewhere.[39] The coordinated water molecules in $Eu^{3+}(tta_n)$@LA was ~3, while the number of water molecules coordinated to the europium ions in the hybrid material $Eu^{3+}(tta_n)$@LA/tpy-IL was calculated to be 0.8. This means that most of the water molecules have been shielded from the first coordination sphere of the Eu^{3+} ions by the synergistic coordination of organic ligand combined with the functionalized ionic liquid.

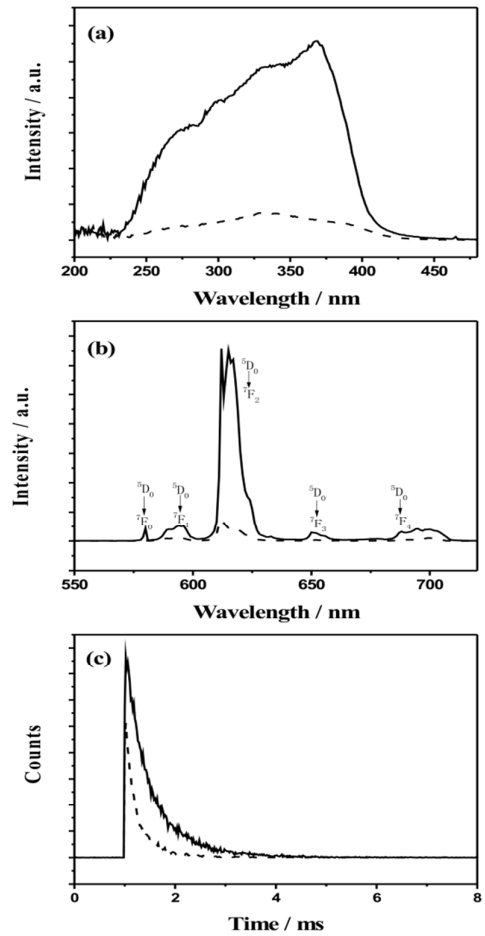

Fig. 6. a) Excitation, b) emission spectra and c) decay curves of $Eu^{3+}(tta_n)$@LA (dotted), $Eu^{3+}(tta_n)$@LA/tpy-IL (solid). The excitation spectra were monitored at 612 nm and the emission spectra were obtained on excitation at 350 nm.

In addition, the intensity ratio of $I(^5D_0 \rightarrow {}^7F_2)/I(^5D_0 \rightarrow {}^7F_1)$ is increased from 6 to 12, indicating the asymmetric coordination field around Eu^{3+} ions, which is due to the strong coordination interaction appearing between the ligands and the Eu^{3+} ions.[40] Moreover, obvious stark splitting (3 lines $^5D_0 \rightarrow {}^7F_2$) can be seen, which further indicates the low-symmetry site occupied by Eu^{3+} ion and a strong ligand field around Eu^{3+} ion. On the other hand, It has been well-documented that the acid environment has significant influence on the luminescence performances of Eu^{3+}-beta-diketonate complexes.[26] TTA ligand can be protonated under acidic environment, which competes with full coordination to Eu^{3+} ions.[27]

We propose that the protons on the Laponite platelets can be removed by addition of tpy-IL through a mechanism of synergic effect of ion exchange and neutralization. This can be supported by the following observations, the suspension of $Eu^{3+}(tta_n)$@LA shows a decrease in pH from～7.3 to ～6.6 after addition of tpy-IL, indicating the releasing of protons from the surface of Laponite by exchanging H^+ with positively charged of tpy-IL. In order to further exploring the luminescence properties of both hybrid materials, the typical decay curves were measured (Fig. 6c). The observed lifetime of $Eu^{3+}(tta_n)$@LA/tpy-IL (0.61ms) is longer than $Eu^{3+}(tta_n)$@LA (0.23ms), which is in coincidence with the results of emission spectra. As expected, the modified materials yield about 7-fold increase in luminescence quantum efficiency.

2.4 Thermal- and photo-stability

Drawbacks such as low thermal [41, 42] and photochemical stability [43] and poor mechanical limit the full exploitation of lanthanide complex in practical application. Hybridize the complexes with stable matrices provide an effective way to overcome the drawbacks.[12, 18, 44-47] In the present work, the thermal- and photo-stability of both materials were studied.

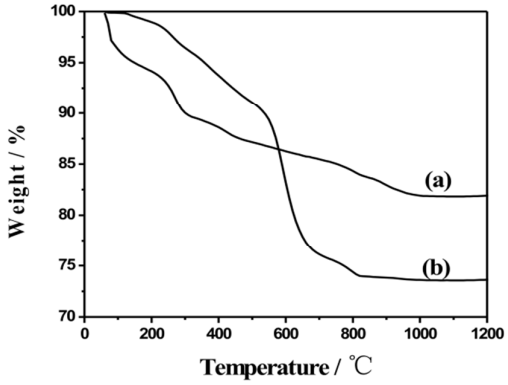

Fig. 7. TG curves of (a) $Eu^{3+}(tta_n)$@LA and (b) $Eu^{3+}(tta_n)$@LA/tpy-IL.

We performed thermogravimetric analysis (TGA) to compare the thermal stability of the $Eu^{3+}(tta_n)$@LA and the $Eu^{3+}(tta_n)$@LA/tpy-IL. Three decomposition stages can be observed in the TG curve of $Eu^{3+}(tta_n)$@LA (Fig. 7a). The first weight loss (6%) below 150 °C could be attributed to the removal of water. The second step, there is a 5% mass loss between 150-330 °C, which corresponds to the dissociation of the tta component. Beyond 330 °C, the Laponite structure also decomposes with a gradual weight loss of 7% and a plateau is developed above 1000 °C. For comparison, the thermal analysis profile of $Eu^{3+}(tta_n)$@LA/tpy-IL is shown in Fig. 7b. Below 150 °C, no obvious weight loss is observed for the TG curve, implying less water molecules coordinated in the complex. This is probably due to the formation of $Eu^{3+}(tta_n)$ with tpy-IL. The weight loss (28%) between 200-480 °C is possibly associated with the degradation of organic moieties from tta and tpy-IL. The Laponite decomposes process is concentrated at narrow temperature range of 480-800 °C, this phenomenon reflected a more regular and orderly structure in $Eu^{3+}(tta_n)$@LA/tpy-IL, which is believed to be ascribed to the enhanced luminescence properties after addition of tpy-IL. As concluded, $Eu^{3+}(tta_n)$@LA/tpy-IL exhibited a higher thermal stability than $Eu^{3+}(tta_n)$@LA.

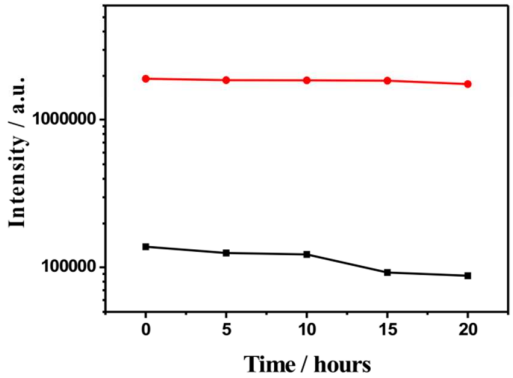

Fig. 8. Changes of the integrated intensity of $^5D_0$ /$^7F_2$ transition after 150 °C heat treatment (holding 0h, 5h, 10h, 15h, 20h); — $Eu^{3+}(tta_n)$@LA; —$Eu^{3+}(tta_n)$@LA/tpy-IL.

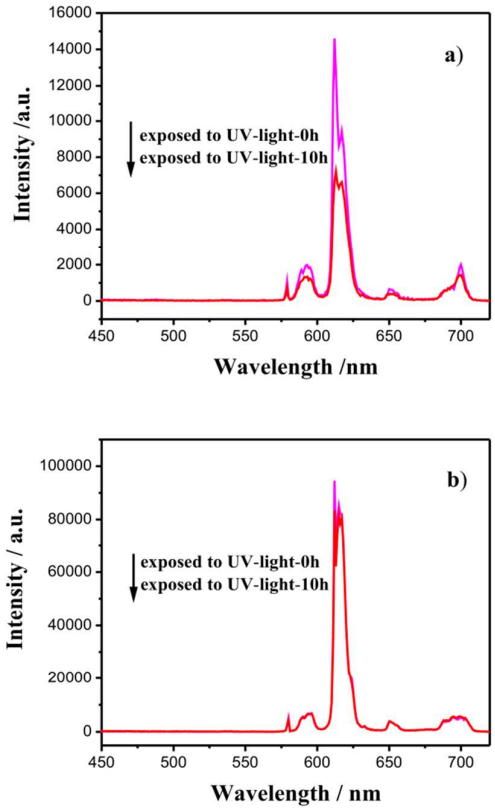

Fig. 9. Emission spectra of a) $Eu^{3+}(tta_n)$@LA and b) $Eu^{3+}(tta_n)$@LA/tpy-IL after exposed to UV irradiation (λ_{ex}=365 nm) (holding 0 h, 10 h) ;

In addition, the thermo-stability of the hybrid materials with and without tpy-IL also was examined by heating at 150 °C under air. The time-dependence profiles of the $^5D_0$ /$^7F_2$ transition integrated intensity are shown in Fig. 8. We observed drastic decrease of emission intensity of $Eu^{3+}(tta_n)$@LA without tpy-IL protection (36%) after 20 h. In contrast, few decrease of the emission intensity of $Eu^{3+}(tta_n)$@LA/tpy-IL was observed, 90% of its original integrated intensity was remained. Photo-stability was investigated by exposing the hybrid materials under ultraviolet lamp. The emission spectra curve of $Eu^{3+}(tta_n)$@LA and $Eu^{3+}(tta_n)$@LA/tpy-IL exposed to UV irradiation for 10 h are shown in Fig. 9. A ~45% decrease in the $^5D_0$/$^7F_2$ transition integrated intensity is observed for $Eu^{3+}(tta_n)$@LA while the value is only ~8% for $Eu^{3+}(tta_n)$@LA/tpy-IL. In summary, pronounced improved thermal-and photo-stability is achieved by incorporation tpy-IL to the hybrid materials. As we can see from the above results, not only because unique properties of the ionic liquid (tpy-IL), but also coordinating ability between europium (Ⅲ) ions and the ligand plays a crucial role in improving the stability of the hybrid materials.

3. Experimental

3.1 Materials

Laponite RD and the alkylamines were purchased from Rockwood Additives Ltd and used as received without further purification. 2-Thenoyltrifluoroacetone (tta) was purchased from Aldrich. Europium chloride ($EuCl_3{\cdot}6H_2O$) was prepared by dissolving Eu_2O_3 into concentrated hydrochloride acid (37%). The excess acid was removed by addition of ethanol followed by successive fuming. The organic salt containing terpyridine moieties (tpy-IL) was synthesized according to the reported procedure.[28]

3.2 Characterizations

X-ray powder diffraction studies were completed with an X-ray powder diffractometer (BRUKER D8 Focus) employing $Cu_{K\alpha}$ radiation (λ=1.5418Å), operating at 40 kV and 40 mA. Infrared (IR) spectra were obtained with a Bruker Vector 22 spectrometer by using KBr pellets for solid samples ranging from 400 to 4000 cm^{-1}. The UV-Vis spectra were recorded on a VARIAN CARY 50 UV-Vis spectrophotometer. Elemental analysis was performed on a Flash EA 1112. SEM images were obtained from a Nova Nano SEM450 at an acceleration voltage of 15 kV. Luminescence spectra were measured on an Edinburgh Instruments model FLS920P spectrometer, with a 450 W Xe lamp as the steady-state excitation source, a double-excitation monochromator (1800 lines mm^{-1}), an emission monochromator (600 lines mm^{-1}), and a semiconductorcooled Hamamatsu model RMP928 photomultiplier tube. Layer charges were estimated from the n-alkylammonium ion-exchange technique[33] and the exchange procedure were operated according to this procedure.[34]

3.3 Preparation of $Eu^{3+}(tta_n)$@LA

On addition of 5 mL $EuCl_3{\cdot}6H_2O$ (0.1mol/L) solutions to 5 wt.% aqueous dispersions of Laponite (0.5g), the mixture was stirred at 80°C for 24 h. The product (denoted as Eu^{3+}@LA) was collected by centrifugation and washed with deionized water several times). The Eu^{3+}@LA was dispersed in 10 mL water; 0.15g of tta dissolved in 5mL of EtOH was then added. After vigorous sonication of the mixture for 2h, the product was collected by centrifugation, washed with EtOH, and dried at 80°C overnight. The product was denoted as $Eu^{3+}(tta_n)$@LA. CHN analysis of $Eu^{3+}(tta_n)$@LA: C 9.002%, H 3.680%.

3.4 Modification of $Eu^{3+}(tta_n)$@LA with tpy-IL

The $Eu^{3+}(tta_n)$@LA was mixed with aqueous solution of tpy-IL in accordance with suitable molar ratio, the mixture was sonicated for 1 h. The product ($Eu^{3+}(tta_n)$@LA/tpy-IL) was then recovered by centrifugation, washed three times with water and dried at 80°C. Characteristic bands of tpy-IL was observed in the FTIR spectra of $Eu^{3+}(tta_n)$@LA/tpy-IL, which indicate the coordination of tpy-IL with Eu^{3+} ions. CHN analysis of $Eu^{3+}(tta_n)$@LA/tpy-IL: C 14.145%, N 1.425%, H 3.614%.

4. Conclusions

In conclusion, we have observed a remarkable increase of luminescence efficiency of a inorganic–organic hybrid material, obtained by loading of Eu^{3+}-beta-diketonate complexes into the Laponite interlayers by a two-step procedure, after modification with tpy-IL. The present of tpy-IL can fully protect Eu^{3+} ions from the water molecule quenching together with remove the abundant protons on the Laponite platelets are believed to be ascribed to the luminescence enhancement. The unique luminescence properties of the hybrid material, together with its good stability and processability, make it highly promising candidate for fabrication of different kinds of optical devices.

Acknowledgements

Financial support by the National Key Basic Research Program (2012CB626804), the National Natural Science Foundation of China (20901022, 21171046, 21271060, and 21236001), the Tianjin Natural Science Foundation (13JCYBJC18400), the Natural Science Foundation of Hebei Province (No.B2013202243), the Program for Changjiang Scholars and Innovative Research Team in University (PCSIRT, IRT1059), and Educational Committee of Hebei Province (2011141,LJRC021) is gratefully acknowledged.

Notes and references

1. T. Jüstel, H. Nikol and C. Ronda, *Angew. Chem. Inter. Ed.*, 1998, **37**, 3084-3103.
2. C. Feldmann, T. Jüstel, C. R. Ronda and P. J. Schmidt, *Adv. Funct. Mater.*, 2003, **13**, 511-516.
3. A. de Bettencourt-Dias, *Dalton Trans.*, 2007, 2229-2241.
4. A. L. Jenkins, O. M. Uy and G. M. Murray, *Anal. Chem.*, 1999, **71**, 373-378.
5. S. V. Eliseeva and J.-C. G. Bünzli, *Chem. Soc. Rev.*, 2010, **39**, 189-227.
6. F. Olivero, F. Carniato, C. Bisio and L. Marchese, *J. Mater. Chem.*, 2012, **22**, 25254-25261.
7. H. Li, M. Li, Y. Wang and W. Zhang, *Chem.- Eur. J.*, 2014, **20**, 10392-10396.

8. S. Lis, Z. Piskula, K. Staninski, S. Tamaki, M. Inoue and Y. Hasegawa, *J.Rare Earths*, 2008, **26**, 185-191.
9. W. Yanli, X. Xianzhu, L. Qianlan, Y. Ruchun, D. Haixin and X. Qiang, *J. Rare Earths*, 2015, **33**, 529-534.
10. Z. Piskuła, J. Czajka, K. Staninski and S. Lis, *J. Rare Earths*, 2014, **32**, 221-225.
11. L. Chen and B. Yan, *Spectrochim. Acta, Part A*, 2014, **131**, 1-8.
12. Y. Wada, M. Sato and Y. Tsukahara, *Angew. Chem. Int. Ed.*, 2006, **45**, 1925-1928.
13. M. Alvaro, V. Fornés, S. García, H. García and J. Scaiano, *J. Phys. Chem. B*, 1998, **102**, 8744-8750.
14. M. I. Stich, S. Nagl, O. S. Wolfbeis, U. Henne and M. Schaeferling, *Adv. Funct. Mater.*, 2008, **18**, 1399-1406.
15. M. Ogawa, T. Nakamura, J.-i. Mori and K. Kuroda, *J. Phys. Chem. B*, 2000, **104**, 8554-8556.
16. T. Nakato, K. Kusunoki, K. Yoshizawa, K. Kuroda and M. Kaneko, *J. Phys. Chem.*, 1995, **99**, 17896-17905.
17. B. Yan and Q.-M. Wang, *Cryst. Growth Des.*, 2008, **8**, 1484-1489.
18. L. D. Carlos, R. A. Ferreira, V. d. Z. Bermudez and S. J. Ribeiro, *Adv. Mater.*, 2009, **21**, 509-534.
19. M. Lezhnina, E. Benavente, M. Bentlage, Y. Echevarria, E. Klumpp and U. Kynast, *Chem. Mater.*, 2007, **19**, 1098-1102.
20. M. E. Hagerman, S. J. Salamone, R. W. Herbst and A. L. Payeur, *Chem. Mater.*, 2003, **15**, 443-450.
21. O.-O. Park and T.-w. Lee, Google Patents, 2003.
22. M. M. Lezhnina, T. Grewe, H. Stoehr and U. Kynast, *Angew. Chem. Int. Ed.*, 2012, **51**, 10652-10655.
23. D. W. Thompson and J. T. Butterworth, *J. Colloid Interface Sci.*, 1992, **151**, 236-243.
24. T. Felbeck, M. Lezhnina, U. Resch-Genger and U. Kynast, *J. Lumin.*, 2014.
25. S. M. Auerbach, K. A. Carrado and P. K. Dutta, *Handb. Layered Mater.*, CRC Press, 2004.
26. M. Lezhnina, M. Bentlage and U. Kynast, *Opt. Mater.*, 2011, **33**, 1471-1475.
27. D. Yang, Y. Wang, Y. Wang, Z. Li and H. Li, *ACS Appl. Mater. Interfaces*, 2015.
28. D. Wang, H. Wang and H. Li, *ACS Appl. Mater. Interfaces*, 2013, **5**, 6268-6275.
29. R. A. Caruso, A. Susha and F. Caruso, *Chem. Mater.*, 2001, **13**, 400-409.
30. J. I. Dawson and R. O. Oreffo, *Adv. Mater.*, 2013, **25**, 4069-4086.
31. T. E. Mallouk and J. A. Gavin, *Acc. Chem. Res.*, 1998, **31**, 209-217.
32. G. Lagaly, *Layer Charge Characteristics of*, 1994, **2**, 1-46.
33. A. Olis, P. Malla and L. Douglas, *Clay Miner.*, 1990, **25**, 39-50.
34. A. Czímerová, J. Bujdák and R. Dohrmann, *Appl. Clay Sci.*, 2006, **34**, 2-13.
35. D. Yang, Y. Wang, Y. Wang, Z. Li and H. Li, *ACS Appl. Mater. Interfaces*, 2015, **7**, 2097-2103.
36. B. V. Lotsch and G. A. Ozin, *ACS nano*, 2008, **2**, 2065-2074.
37. P. Zhang, Y. Wang, H. Liu and Y. Chen, *J. Mater. Chem.*, 2011, **21**, 18462-18466.
38. R. López, D. Villagra, G. Ferraudi, S. Moya and J. Guerrero, *Inorg. Chim. Acta*, 2004, **357**, 3525-3531.
39. M. Fernandes, V. de Zea Bermudez, R. Sá Ferreira, L. Carlos, A. Charas, J. Morgado, M. M. Silva and M. J. Smith, *Chem. Mater.*, 2007, **19**, 3892-3901.
40. S. Tang, A. Babai and A. V. Mudring, *Angew. Chem. Inter. Ed.*, 2008, **47**, 7631-7634.
41. Y. Wang, H. Li, L. Gu, Q. Gan, Y. Li and G. Calzaferri, *Microporous Mesoporous Mater.*, 2009, **121**, 1-6.
42. D. Yang, J. Wang and H. Li, *Dyes Pigm.*, 2015, **118**, 53-57.
43. T. Pagnot, P. Audebert and G. Tribillon, *Chem. Phys. Lett.*, 2000, **322**, 572-578.
44. J. Feng and H. Zhang, *Chem. Soc. Rev.*, 2013, **42**, 387-410.
45. K. Lunstroot, K. Driesen, P. Nockemann, L. Viau, P. H. Mutin, A. Vioux and K. Binnemans, *Phys. Chem. Chem. Phys.*, 2010, **12**, 1879-1885.
46. L. Carlos and R. S. Ferreira, in *Hybrid Nanocomposites for Nanotechnology*, Springer, 2009, pp. 509-586.
47. C. Peng, H. Zhang, J. Yu, Q. Meng, L. Fu, H. Li, L. Sun and X. Guo, *J. Phys. Chem. B*, 2005, **109**, 15278-15287.